Journal of Lasers in Medical Sciences

J Lasers Med Sci 2024;15:e40

Original Article

http://journals.sbmu.ac.ir/jlms

doi 10.34172/jlms.2024.40

The Application of Photobiomodulation and Stem Cells Seeded on the Scaffold Accelerates the Wound Healing Process in Mice

Masoumeh Hajihosseintehrani[1], Abdollah Amini[1*], Mohammadhossein Heidari[1], Mazaher Gholipourmalekabadi[2], Fatemeh Fadaei Fathabady[1], Atarodalsadat Mostafavinia[3], Houssein Ahmadi[1], Maryam Khodadadi[4], Reza Naser[5], Fateme Zare[1], Sanaz Alizadeh[3], Nafiseh Moeinian[1], Sufan Chien[6], Mohammad Bayat[2,6*]

[1]Department of Biology and Anatomical Sciences at Shahid Beheshti University of Medical Sciences (SBMU), Tehran, Iran
[2]Department of Tissue Engineering & Regenerative Medicine, Iran University of Medical Sciences, Hemmat Highway, Tehran, Iran
[3]Department of Anatomical Sciences and Cognitive Neuroscience at the Faculty of Medicine, Tehran Medical Sciences, Islamic Azad University, Tehran, Iran
[4]Xi'an jiaotong University School of Stomatology, Xi'an, Shaanxi Province, China
[5]Tissue Engineering Department, School of Advanced Technologies in Medicine, Tehran University of Medical Sciences, Tehran, Iran
[6]Price Institute of Surgical Research at the University of Louisville and Noveratech LLC of Louisville in Louisville, KY, USA

***Correspondence to**
Abdollah Amini,
Email: d.amini2008@yahoo.com
and Mohammad Bayat,
Email: bayat_m@yahoo.com

Received: March 3, 2024
Accepted: May 8, 2024
ePublished: August 14, 2024

Abstract

Introduction: The purpose of this research was to test the impact of seeding a hydrogel chitosan scaffold (HCS) with human adipose-derived stem cells (hADSCs) under the influence of photobiomodulation (PBM) on the remodeling step on the wound repairing process in mice.

Methods: Thirty mice were randomly assigned to five groups (n=6 per group): The control group (group 1) consisted of mice without any intervention. In group 2, an HCS was implanted into the wound. In group 3, a combination of HCS+hADSC was inserted into the wound. In group 4, an HCS was inserted into the wound and PBM was applied. In group 5, a combination of HCS+hADSCs was inserted into the wound, followed by PBM treatment.

Results: Improvements in the injury closing rate (WCR) and microbial flora were observed in all groups. However, the highest WCRs were observed in group s 5, 4, 3, and 2 (all *P* values were 0.000). Groups 3-5 showed increased wound strength compared to group s 1 and 2, with group 2 demonstrating better results than group 1 (*P* values ranged from 0.000 to 0.013). Although group s 3-5 showed increases in certain stereological elements compared to group s 1 and 2, group 2 exhibited superior results in comparison with group 1 (*P* values ranged from 0.000 to 0.049).

Conclusion: The joined use of HCS+hADSCs+PBM significantly accelerated the wound healing process during the maturation phase in healthy mice. This approach demonstrated superior wound healing compared to the use of HCS alone, hADSCs+HCS, or PBM+HCS. The findings suggest an additive effect when HCS+hADSCs+PBM are combined.

Keywords: Hydrogel chitosan scaffold; Human adipose-derived stem cells; Photobiomodulation; Wound healing process; Mice.

Introduction

A wound is an injury to the skin that can result in pain and susceptibility to infection.[1] Acute wounds, such as surgical or traumatic wounds, abrasions, or superficial burns, are commonly encountered.[2] However, some acute wounds exhibit impaired healing, leading to delayed healing and a state of pathologic inflammation.[3] Each year, millions of people worldwide are affected by delayed acute wounds, which occur when the normal healing process is disrupted.[4]

Over the earlier two decades, regenerative medicine and skin tissue engineering (STE) have made significant progress in restoring and reconstructing damaged tissues, including the skin. Researchers have explored various techniques, such as three-dimensional structured scaffolds, hydrogels, and growth factors, to facilitate the improvement of practical engineered materials and

Please cite this article as follows: Hajihosseintehrani M, Amini A, Heidari M, Gholipourmalekabadi M, Fadaei Fathabady F, Mostafavinia A. The application of photobiomodulation and stem cells seeded on the scaffold accelerates the wound healing process in mice. *J Lasers Med Sci.* 2024;15:e40. doi:10.34172/jlms.2024.40.

deliver necessary provisions throughout implantation in living organisms.[5,6] Various techniques have been researched to accelerate skin regeneration in STE.[7,8] The STE process often involves constructing a scaffold from different materials, followed by the introduction of cells with or without photobiomodulation (PBM) or growth factors to promote tissue development.[9,10] The main goal of STE is to fully recover the structural and functional characteristics of a wounded area to its original state prior to the injury.[8] However, STE currently has limited applications in patient treatment, as the procedures are experimental and expensive, and only a subset of healing purposes can be repaired.[11]

Mesenchymal stem cells (MSCs) play a role in promoting the healing of chronic ulcers during every phase of the wound healing process. One significant aspect of MSCs is their ability to shorten the duration of the prolonged inflammatory stage.[12]. Stem cells, particularly adipose-derived stem cells (ADSCs), show a vital role in STE as they have shown effectiveness in developing new treatments.[13,14] ADSCs undergo cellular division and transformation into skin cells in order to restore injured cells. Additionally, they stimulate the regeneration of cells and facilitate the recovery process by means of autocrine and paracrine mechanisms.[15] Recent studies have shown the positive effects of MSCs in combination with the denatured acellular dermal matrix or photobiomodulation (PBM) on wound healing in mice. [16,17] However, the harsh injury location limits the engraftment, preservation, and endurance rate of transplanted MSCs.[18] Various approaches have been explored to enhance the therapeutic potential of MSCs, such as using different scaffolds to facilitate MSC delivery and migration into the wound.[19]

PBM via near-infrared and red light has emerged as a hopeful drug-free method for helping injury repair, reducing inflammation, alleviating pain, and restoring action. The capability of these lights to enter tissue and definitely moderate molecular and biochemical reactions has contributed to their effectiveness.[20] Latest studies have revealed the positive effects of PBM on MSCs,[21] as well as its ability to modulate antioxidant levels in ADSCs.[21]

Hydrogels, specifically those composed of chitosan, have exhibited potential as effective wound dressings due to their compatibility with living tissue, ability to break down naturally, high water absorption capacity, and water retention properties. Chitosan is a biomaterial derived from chitin through deacetylation and possesses advantageous characteristics such as easy availability, antibacterial and blood clotting abilities, and the capability to facilitate skin regeneration. By combining chitosan hydrogels with blood clots and PBM, there is the possibility to enhance dental pulp regeneration by utilizing cell homing techniques.[22] In an experimental work directed by Moreira et al in 2021, it was hypothesized that an experimental injectable chitosan hydrogel could promote the spatial arrangement of endogenous MSCs in the regeneration of dental pulp without impeding the positive effects of PBM.[23] The tested chitosan hydrogel in their research demonstrated significantly increased proliferation, migration, and viability of MSCs in laboratory settings while PBM was used, and this was consistent with the findings observed in live subjects.[23]

In this study, we successfully implanted an HCS combined with hADSCs into an injury site under the influence of PBM on the remodeling phase of injury repairing in mice. We hope that our findings can pave the way towards a novel approach for effectively treating non-healing wounds and ulcers in patients.

Materials and Methods

Study Design and Animals

Thirty adult male Naval Medical Research Institute (NMRI) mice, aged 3.5 months and weighing around 25 g, were obtained from the Pasteur Institute of Iran, the Production and Research Complex in Tehran. The animals were separately housed in standard cages and fed with standard mice food pellets from Behparvar Co. in Tehran, Iran. Subsequently, they were randomly divided into five groups, with each group consisting of six mice.

In this experiment, we first utilized non-invasive methods, including the application of acid dyes to mark the tail and back skin of mice for grouping purposes. Following this, the rats were housed in cages labeled with the group name, date, and researcher's name.[24]

Group one served as the control group without any interventions. In group two, a hydrogel chitosan scaffold (HCS) was inserted into the wound. In group three, an HCS combined with hADSCs was inserted into the wound. In group four, an HCS was inserted into the wound, and the wound was subjected to PBM. In group five, an HCS combined with hADSC was inserted into the wound, and the wound was subjected to PBM. On days 0, 8, and 16, the wound closure rate (WCR) and microbiological examinations were performed. Throughout the duration of the study, the weight of the mice was consistently tested. On the 16th day, the mice were humanely put to sleep, and the samples were taken for further analysis by using tensiometrical and stereological methods.

Synthesis of Hydrogel Chitosan Scaffold

A 2% (w/v) solution of medium molecular weight chitosan was solved in the solution of acetic acid (0.1 mol/L) and stirred for 24 hours at 25 °C. The solution was then centrifuged for 5 minutes at 3000 × g. A 40% (w/v) solution of β-glycerol phosphate (β-GP), used as a cross-linker, was provided and filtered by a 0.22 μm filter. The β-GP solution was gradually added to the chitosan hydrogel while stirring for 15 minutes at 4 °C. The thermosensitive property of the hydrogel was examined

by a tube formation assay at 4 °C, 25 °C, and 37 °C.[25,26]

Characterization of the Hydrogel Chitosan Scaffold

The morphology of the synthesized thermosensitive hydrogel was controlled under a scanning electron microscope (VEGA3, TESCAN, Czech Republic). For scanning electron microscopy (SEM) analysis, the samples were covered with a tinny coating of gold nanoparticles by the sputter-coating method and checked under SEM at an accelerated voltage of 15 kV. For the swelling assay, the dry samples were weighed, submerged in phosphate-buffered saline for about one hour at 37 °C, and then removed. The weights of the samples were immediately determined and measured again 5 minutes after blotting onto filter paper to remove excess water. The swelling ratio was determined by applying the following formula: Swelling ratio (in percent) = ((Ww - Wd) / Wd) × 100, where Ww denotes the weight of the expanded scaffolds and Wd corresponds to the weight of the initial dry scaffolds.[25]

Isolation, Expansion, and Immunophenotyping of hADSCs

Adipose tissue was achieved from an adult female undergoing cosmetic breast surgery with informed consent. Almost 5 cc of adipose tissue was separated, cultured, and expanded following standard methods. The MSC markers of the cells were assessed by using flow cytometry, following a methodology previously documented in a report.[27]

hADSC Seeding and Transplantation

Immediately after surgery, 1×10^6 passage 4 hADSCs[21] were seeded onto an 8-mm diameter HCS, and the scaffold was transplanted into the wounds of the mice in group s 3 and 5 (Figure 1).

Surgery

Using a standard punch (as shown in Figure 1), an 8-mm diameter circular skin injury was surgically made on the upper portion of the animal's backs. The procedure was performed under sterile conditions while the mice were under general anesthesia.[28] After PBM therapy, the wounds were initially dressed with a Vaseline dressing and then covered with a cotton dressing. Finally, the wound area was covered with leukoplast tape. The mice were monitored daily, and the dressings were checked regularly.

Photobiomodulation

In group s 3 and 5, the wounds and their adjacent areas were subjected to PBM on days 4, 8, 12, and 16 while the mice were under general anesthesia. The specifications of the laser used are reported in Table 1.[28,29]

Measurement of the Wound Closure Rate

Photographs of the wounds were captured by using a digital camera, and the surface site was calculated by means of ImageJ-NIH software (USA). The WCR for each injury was calculated by the following formula:

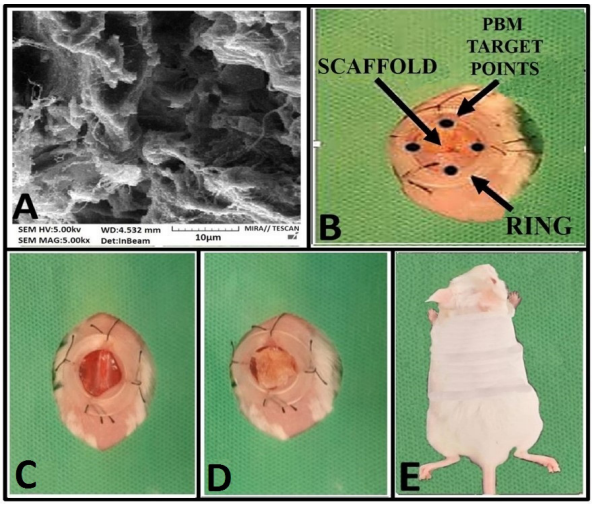

Figure 1. hADSC Seeding and Transplanting after surgery. Panel A: Scanning electron microscopic photo of a wet hydrogel chitosan hydrogel. Panel B: An image of the wound, ring, laser spots, and scaffold. Panel C: wound area, Panel D: Scaffold, Panel E: Wound area was covered by a Vaseline dressing and leukoplast tape which was circled around the thoracic region of the mice

[(Surface area at day zero - Surface area at day X) / Surface area at day zero] × 100%

Microbiological Test

Swabs were provided from the wounds of the animals on days zero, 8, and 16. The samples were analyzed by using standard methods to detect *Pseudomonas aeruginosa* as a gram-negative bacteria and *Staphylococcus aureus* or *Staphylococcus epidermidis* as gram-positive bacteria. Müller-Hinton Agar was used to detect all the mentioned bacteria, and the Mannitol salt culture medium was used to differentiate between *S. aureus* and *S. epidermidis*. The microbial numbers in each sample of the wounds were quantified as the colony-forming unit (CFU).[30]

Tensiometrical Test

Rectangular samples, with dimensions of 3 mm × 30 mm, were obtained from the wounds by using a conventional dual-blade cutting tool. These samples were attached to a material testing device (SANTAM, Iran) and subjected to a constant deformation rate of 10 mm/min. The bending stiffness (expressed in MPa) was calculated by dividing the maximum force by the displacement at the point of rupture. The stress under a high load (in N/mm^2) was determined by dividing the maximum force by the cross-sectional area of the sample.[28]

Stereological Examination Using the Physical Dissector Method

To numerical density (Nv) evaluation of fibroblasts,

Table 1. Treatment Parameters of Photobiomodulation

Parameter (Unit)	Value
Beam spot size at target (cm^2)	0.14
Irradiance at target (mW/cm^2)	0.00625
Exposure duration (s)	800
Energy density or radiant exposure [J/cm^2] for one and 4 shootings	13.84, 55.36
Average radiant power: W × time = energy [J] for one spot (point)	0.001 × 0.8 = 0.8
Number of points irradiated for one wound	4
Area irradiated (cm^2)	3.24
Application technique	Tip of the LO7 probe was positioned vertically close to the target
Number and frequency of treatment sessions, energy density (J/cm^2), or radiant exposure	5 sessions, one time, every 4 days, 276.8
Total radiant energy [J] for one session and 5 sessions	3.2, and 1.6
Exposure duration (s)	800

neutrophils, and macrophages in the wound tissue samples, histological examination was conducted on 10 sections with a width of 5 µm. These slices were stained by the hematoxylin and eosin (H&E) technique. A total of six fields per section were randomly observed under a Nicon light microscope from Japan, with a magnification of 40 × 10.

The calculation for the total surface area tested in all the slices from each rat can be performed by using the following formula:

Total surface area = 10 (sections) × 6 (fields) × 6 × 6.25 mm^2 (surface area of each field at a magnification of 40 ×)

Substituting the Values

Total surface area = 10 × 6 × 6 × 6.25 mm^2

Total surface area = 2250 mm^2.

Therefore, the total surface area tested in all the slices from each rat is 2250 mm^2.

To calculate Nv, we summed up (ΣQ) the cell number (nuclei) for each type of cell. This value was then divided by the height of the dissector (h), multiplied by the area/field (counting frame area), and further multiplied by the total number of the counting frames in all fields (Σp).

The total cell count in each sample (N) was obtained by multiplying Nv by the total volume (V).

Assessment of Vascular Length (as a Biomarker for Angiogenesis)

Measuring the length of blood vessels can serve as a potential biomarker for assessing angiogenesis.

This can be calculated using the formula:

Vascular Length = Total number of vessels counted per rat / (Number of counting frames in all fields * ratio of area to field).

To estimate the volumes of new epidermis and dermis, we can employ Cavalieri's method. The formula is as follows:

Volume = Total number of points counted per sample * (Area/Point) * Thickness.

In the above equations, ΣQ represents the total number of vessels counted per rat, ΣP denotes the number of counting frames in all fields, a/f refers to the ratio of area to field, Σp signifies the total number of points counted per sample, a/p represents the ratio of area to point, and *t* represents the thickness.[31]

Statistical Analysis

Data representation involved the use of mean and standard deviation (SD). The normality of the data was assessed through the Shapiro test. To analyze the data, we employed the student t-test, one-way analysis of variance (ANOVA), and least significant difference (LSD) tests. Statistical significance was determined at a *P* value of less than 0.05.

Results

Mechanical and Swelling Tests

Table 2 displays the outcomes of the mechanical and swelling tests of the HCS. It presents the average values, along with standard deviations for various weights obtained during the mechanical test, as well as the swelling ratio of the CHS in the diverse groups under examination. The data underwent analysis through the student t test, and the significance levels are represented by asterisks (* $P < 0.05$, ** $P < 0.010$, *** $P < 0.000$).

Marker Expression

The cluster of differentiation (CD) 34, CD90, and CD105 were expressed by more than 97% of the hADSCs. Approximately 87.2% of the hADSCs expressed CD73, while CD11b was expressed by 11.8%, and only 0.68% expressed CD45.

Clinical Observations

Based on the clinical observations, it was found that there was no injury exudate present in any of the injuries in the examined groups. This suggests that there was no

Table 2. Mean ± Standard Deviation of the Mechanical and Swelling Tests of the Hydrogel Chitosan Scaffold in Study Groups on the Surgery (Day 1), (Day 4), (Day 8), and Sampling Times (Day 16)

Test	Day	First Weight	Second Weight	*P* Value
Mechanical	Day 1	0.0373 ± 0.008*	0.0207 ± 0.009	< 0.05
Mechanical	Day 4	0.0443 ± 0.0146**	0.0247 ± 0.014	< 0.01
Mechanical	Day 8	0.0407 ± 0.007**	0.0183 ± 0.008	< 0.01
Mechanical	Day 16	0.0317 ± 0.009*	0.0137 ± 0.010	< 0.01
Swelling ratio		Results between the first and second measurements 271.2 ± 19.6***	Results between the first and third measurements 164.6 ± 12.0	< 0.000

excessive discharge or fluid accumulation at the surgical sites.

Additionally, there were no important changes in body weights among the examined groups on days 0 and 16 after surgery. This indicates that the interventions or treatments being studied did not have a notable impact on the body weights of the subjects during this period ($P > 0.05$) (Table 3).

Findings WCR

While all statistical results are shown in the Figure 2, Panels 2A and 2B, we only reported significant differences without mentioning "significant." All *P* values were obtained from the LSD test. There were increases in WCR from day four towards day 16 in all studied groups (all *P* values: $P = 0.000$) (Panel 2A). On all studied days, the groups with the highest WCRs were groups 5, 4, 3, and 2 (all *P* values were equal to 0.000) (Panel 2B).

Microbiological Results

All results are shown in Figure 3. There were decreases in CFUs of *S. epidermis* from day 8 towards day 16 in all studied groups (all *P* values = 0.000) (Figure 3A). There were significant decreases in CFUs of *S. epidermis* in groups 1-3 compared to groups 4 and 5 on day 8 (all *P* values: $P = 0.000$) (Figure 3B). On both days 8 and 16, the lowest CFUs belonged to groups 2 and 3 (*P* values ranged from 0.018 to 0.000) (Figure 3B).

Tensiometrical Results

As shown in the Figure 4 A, group s 3-5 exhibited increased bending stiffness compared to groups 1 and 2, with statistical significance (*P* vvalues: 0.003, 0.003, 0.000 and 0.007, 0.006, 0.000, respectively). Group 5 showed superior results compared to groups 4 and 3 (both *P* vvalues: 0.009) (Fig. 4A). The noticeable levels are labeled as follows: * $P < 0.05$, ** $P < 0.013$, *** $P < 0.000$.

Stress High Load

Groups 2-5 demonstrated an improved stress high load compared to group 1, with statistical significance (*P* values: 0.000). The *P* value between groups 1 and 2 was 0.001. Groups 3-5 exhibited an increased stress high load compared to group 2 (*P* values: 0.013, 0.011, and 0.000). The results of group 5 were superior to groups 4 and 3 (*P* values: 0.005, 0.004) (Figure 4B).

Table 3. Mean ± Standard Deviation of Body Weights of Mice in Study Groups on the Surgery (Day 0) and Sampling Times (Day 16)

Groups	Days		*P* value
	DAY 0	DAY16	
Control	25.2 ± 5.6	25.2 ± 4.8	> 0.05
Scaffold	25.7 ± 4.0	26.0 ± 3.5	> 0.05
Scaffold + Cell	26.0 ± 3.9	27.0 ± 3.5	> 0.05
Scaffold + PBM	23.0 ± 3.1	24.2 ± 4.1	> 0.05
Scaffold + Cell + PBM	24.5 ± 4.6	26.7 ± 4.5	> 0.05

PBM, Photobiomodulation.

Histological and Stereological Results

Figure 5 displays illustrative histological pictures of the wound regions in the five experimental groups on day 16. The examination revealed no notable variances in neutrophil counts among the groups under investigation (Figure 6A).

Macrophages

There were fewer macrophages in group 5 compared to groups 1, 2, 3, and 4 (*P* values: 0.000, 0.000, 0.001, 0.002) (Figure 6B).

Proliferative Elements, Fibroblasts

From a stereological perspective, groups 2-5 exhibited increased fibroblast counts compared to group 1 (*P* value: 0.000). The *P* value between groups 1 and 2 was 0.001. Groups 3-5 demonstrated increased fibroblast counts compared to group 2 (all *P* values: 0.000). Results of groups 5 and 4 were superior to group 3 (*P* values: 0.000, 0.004). Group 5 showed higher counts compared to group 4 (*P* value: 0.000) (Figure 6C).

Angiogenesis

Groups 2-5 exhibited increased angiogenesis compared to group 1 (all *P* values: 0.000). The *P* value between groups 1 and 2 was 0.029. Groups 3-5 demonstrated significant increases in angiogenesis compared to group 2 (*P* values: 0.020, 0.002, and 0.000). The results of group 5 were superior to groups 4 and 3 (both *P* values: 0.000) (Figure 6D).

Volumes of New Epidermis and New Dermis

While there were similar patterns of changes in the volumes of new epidermis and new dermis among the studied groups, statistical differences were reported for both as new volumes of epidermis and dermis (ED). New volumes of ED in group s 5-2 were higher than in group 1 (all *P* values = 0.000). Concurrently, the *P* value between groups 1 and 2 in volume on the new epidermis was equal to 0.049, and the *P* value between group s 1 and

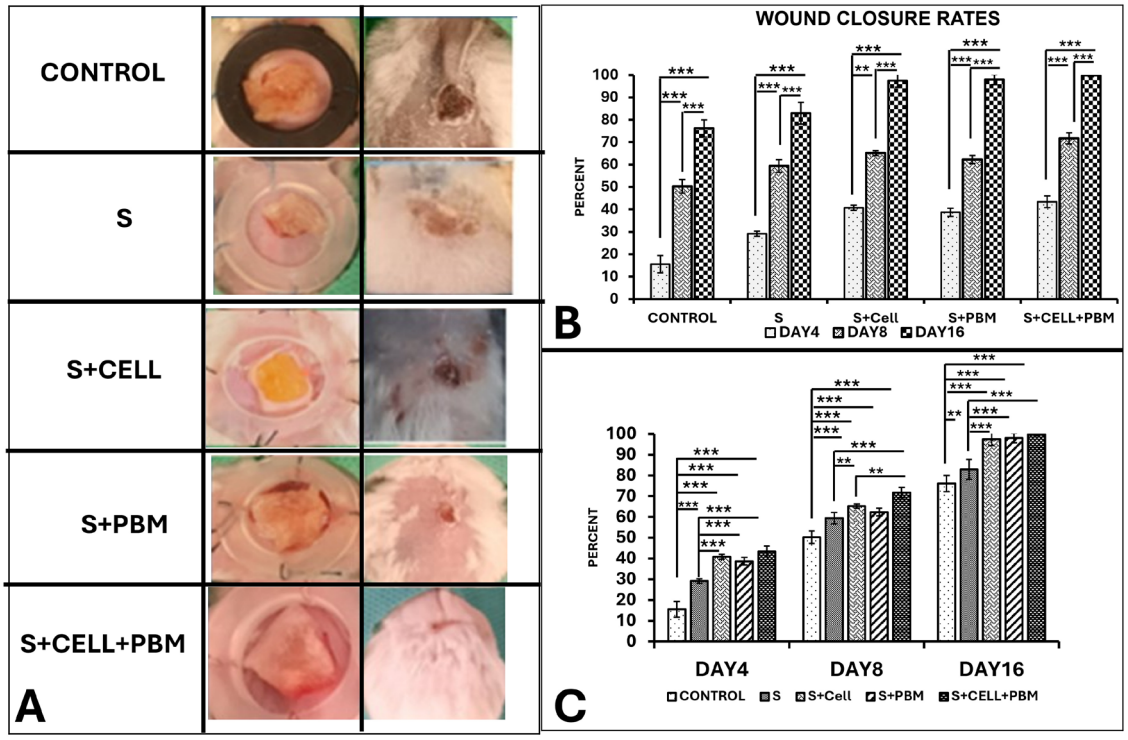

Figure 2. The size of the wound area in studied groups on days of 0 to16th. Panel A illustrates the progressive and enhanced healing process of wounds across the five study groups, as observed over a specific duration. Panel B compares the mean ± SD of the wound closure rate for each group on days 4, 8, and 16, using ANOVA and LSD tests. Panel C compares the mean ± SD of the wound closure rate among groups on each day (days 4, 8, and 16) using ANOVA and LSD tests. *** $P < 0.000$. Description of groups: G1was control group without any intervention; G 2: hydrogel chitosan scaffold (S) was inserted in the wound; G3, S+CELL: An S + human adipose derived stem cells were inserted in the wound. G4, S+PHOTOBIOMODULATION (PBM): An S was inserted in the wound, and the wound was subjected to PBM. G5: S+CELL+PBM: An S + CELL was inserted in the wound, and the wound was subjected to PBM.

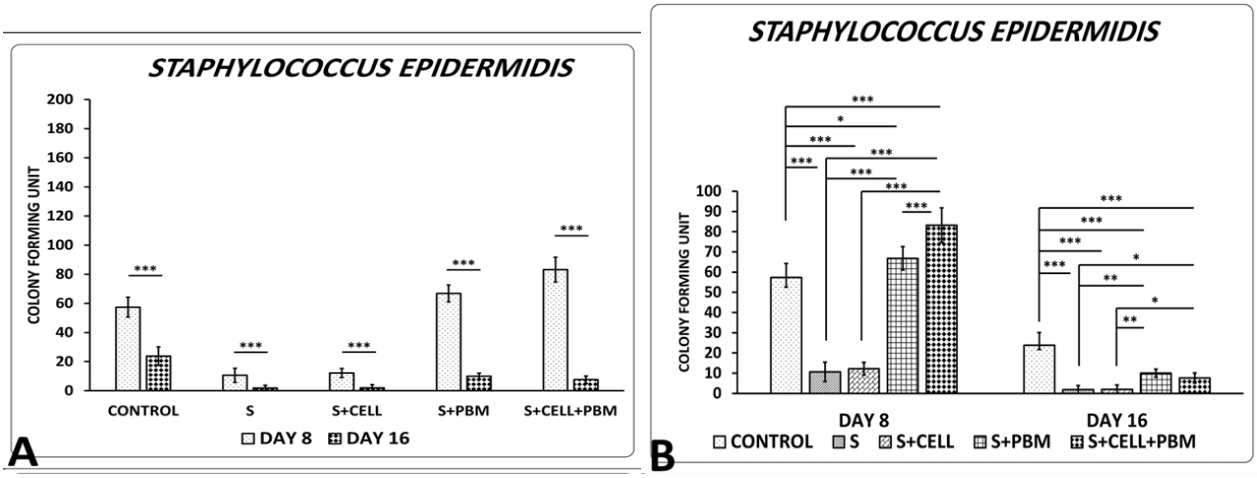

Figure 3. The count of colony-forming units (CFU) in experimental and control groups on the days of 8th and 16th. Panel A compares the mean ± SD of colony-forming units (CFUs) of S. epidermis between days 8 and 16 in each group using ANOVA and LSD tests. Panel B compares the mean ± SD of CFUs of S. epidermis on days 8 and 16 among groups using ANOVA and LSD tests.

2 in volume on the new dermis was equal to 0.011. New volumes of ED in group s 5-3 were higher than in group 2 (all P values = 0.000). New volumes of ED in group 5 were higher than in group s 4 and 3 (all P values = 0.000) (panels E and F of Figure 6).

Discussion

In our study, significant improvements were observed in the WCR and microbial flora from day zero to day 16 in all groups ($P = 0.000$). The highest WCRs were consistently observed in groups 5, 4, 3, and 2 ($P = 0.000$ for most comparisons). Furthermore, groups 3-5 exhibited increased wound strength compared to groups 1 and 2, with group 2 showing better results than group 1 (P values ranged from $P = 0.000$ to $P = 0.013$). Group 5 had fewer macrophages compared to the other groups ($P = 0.000$ to $P = 0.002$). Additionally, groups 3-5 showed increased fibroblasts, angiogenesis, volumes of new epidermis, and

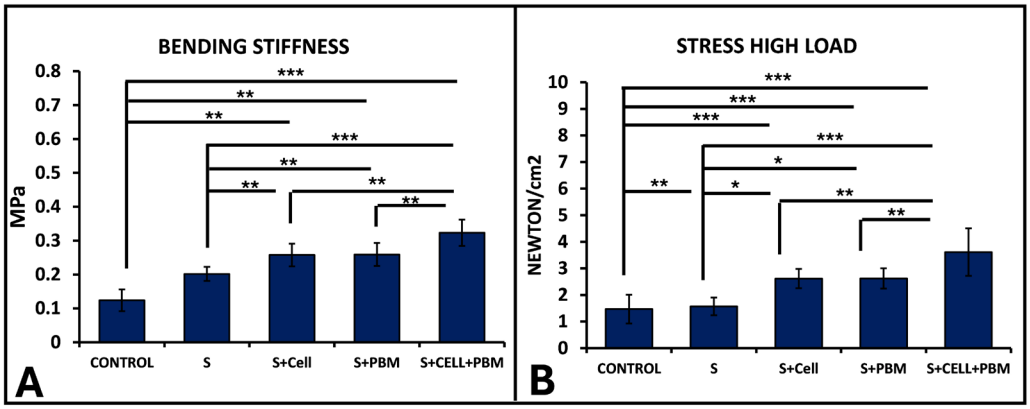

Figure 4. Comparison of bending stiffness and stress high load level in the studied groups on days 16. Panel A presents a comparison of the average ± SD (standard deviation) for bending stiffness among the groups examined using ANOVA and LSD tests. The levels of significance are denoted as follows: * indicates $P < 0.05$, ** indicates $P < 0.01$, and *** indicates $P < 0.000$. In Panel B, the average ± SD for stress under high load is compared among the studied groups using ANOVA and LSD tests. The significance levels are once again indicated as * for $P < 0.05$, ** for $P < 0.01$, and *** for $P < 0.000$.

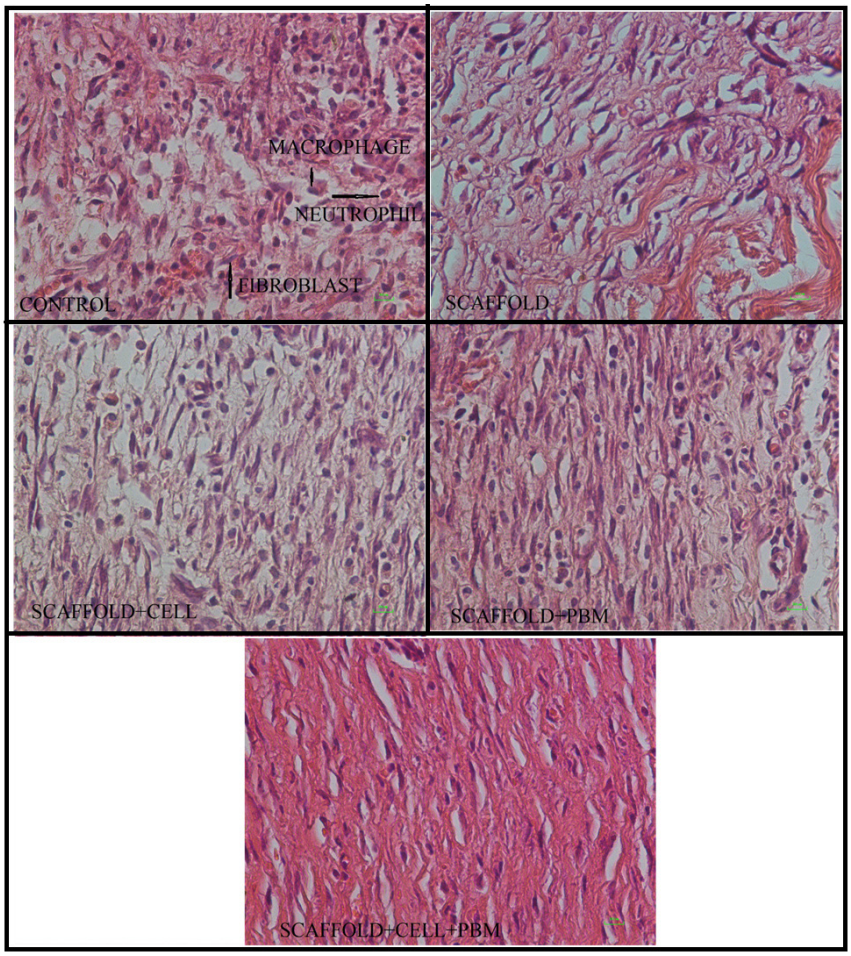

Figure 5. Histological images of the injury sites from the five experimental groups. On day 16, Hematoxylin Eosin and staining was considered to get typical histological pictures of the injury sites from the five experimental groups. The images depict various cellular components such as fibroblasts (F), macrophages (M), neutrophils (N), and blood vessels (V). The magnification used for capturing these images was 40×10.

new dermis compared to groups 1 and 2, with group 2 outperforming group 1 (P values ranged from $P = 0.000$ to $P = 0.049$).

The impact of poor wound healing on the quality of life is significant, affecting approximately 2.5% of the US population. Wound management also has a considerable economic impact on healthcare.[32] STE approaches, particularly those involving stem cell therapy, have shown promise in improving wound healing rates and regenerating the skin.[33] Nonetheless, the clinical utilization of transplanted stem cells faces hurdles due to the limited viability of the cells at the specific injury location, as well as

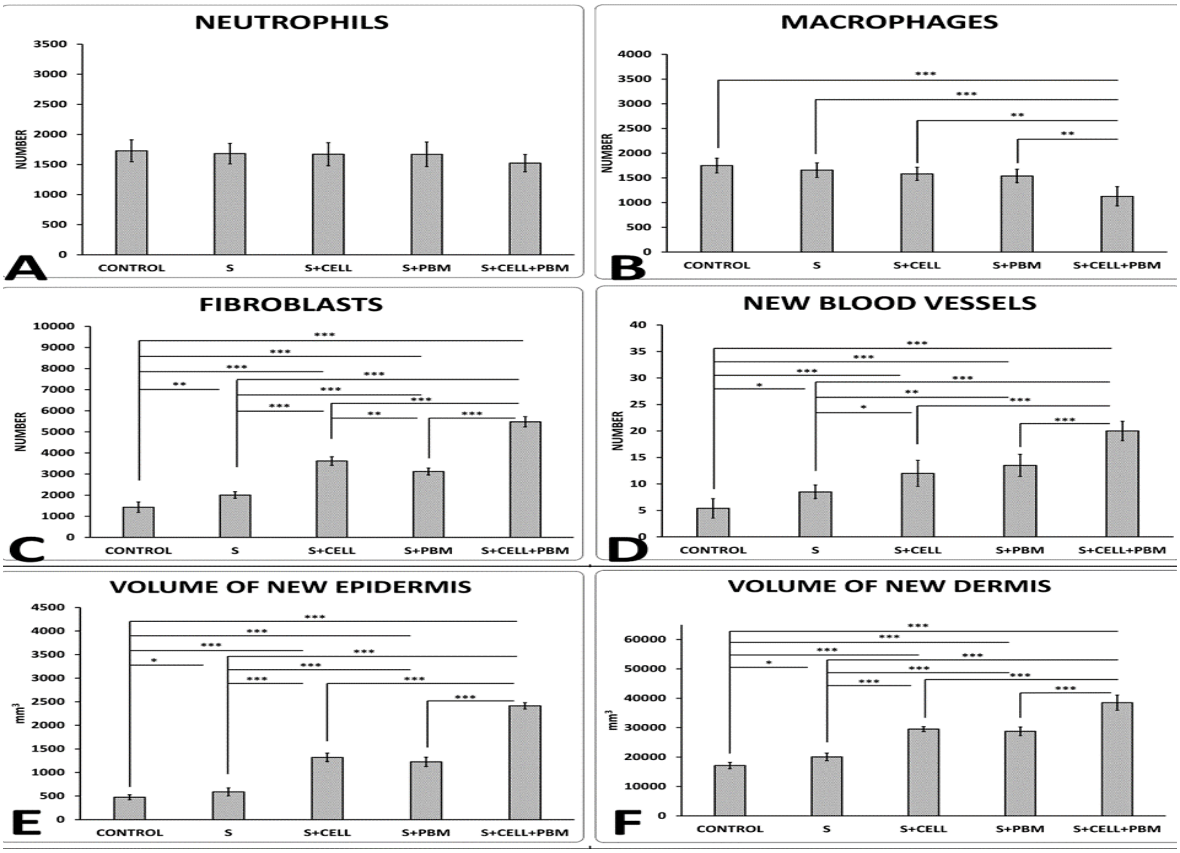

Figure 6. The stereological findings, among the studied groups on day 16. The comparison of mean±SD of neutrophils count (panel A), macrophages count (panel B), fibroblasts count (panel C), new blood vessels (angiogenesis) count (panel D), volumes of new epidermis (panel E), and new dermis (panel F) between the studied groups by using ANOVA and LSD tests. **P*<0.05, ***P*<0.010, ****P*<0.000.

their susceptibility to immune responses and diminished rates of survival, proliferation, and differentiation.[34] Biomaterials can help overcome these barriers and are commonly used in combination with stem cells for STE in injury repair treatments.[34]

The integration of stem cells into organized and developed biomaterials improves the healing and repair of damaged skin tissue, leading to enhanced injury repair factors such as better epithelialization, formation of granulation tissue, increased vascularization, and promotion of angiogenesis.[34-36]

In an animal model of skin damage, MSCs have demonstrated the ability to reduce inflammation by lowering the levels of neutrophils and macrophages, as well as pro-inflammatory cytokines such as IL-1, IL-6, and TNF-α, while increasing anti-inflammatory cytokines like IL-10 and VEGF. This decrease in inflammation has been linked to a reduction in hypertrophic scarring. MSCs can transform macrophages from an inflammatory state to an anti-inflammatory state, which promotes wound healing and decreases MMP-9 levels. Furthermore, MSCs can release substances like VEGF that encourage angiogenesis and support the development of endothelial progenitor cells. Research has indicated that MSCs can travel to wound sites and evolve into various cell types, including keratinocytes and endothelial cells. Various sources of MSCs, such as bone marrow, adipose tissue, umbilical cord, and placenta, have been employed in treating diabetic wounds, each displaying different levels of differentiation potential and pro-angiogenic characteristics. Additionally, extracellular vesicles derived from MSCs have been found to aid in skin cell proliferation and angiogenesis.[12]

In the current study, the results of groups 2 (HCS) and 3 (HCS + hADSCs) align with previous research indicating that the application of chitosan dermal scaffold alone,[37] collagen + chitosan scaffold,[38] or chitosan + hADSCs[37] can induce the rapid growth and maturation of blood vessels during injury repair and cause the healing of full-thickness injuries and the making of an organization similar to a typical skin. Furthermore, these treatments improve injury repair and promote the differentiation of endothelial, fibro-vascular, and epithelial components in the renovated tissue.[37,39]

To our current understanding, there have been no investigations conducted on the impact of PBM therapy on a hybrid approach involving both scaffold and stem cells within a simulated model of skin wound healing. However, some other studies have successfully examined the combination of scaffold + stem cells + PBM in a

femoral critical-size defect simulation in healthy and osteoporotic rats. In osteoporotic rats, the combination of HCS + PBM + ADSCs was superior to other protocols, significantly improving the repairing of critical-size femoral deficiencies in ovariectomized rats and affecting the expression of some related genes. [40-42] In healthy rats, ADSC preconditioning with PBM in vitro + PBM in vivo + HCS meaningfully improved bone strength, stereological parameters, and several important mRNA gene expressions during bone repair.[43-45] It was concluded that ADSCs play an important role in skin wound repair due to their benefits, such as immune compatibility and lack of ethical constraints.[31,46]

While significant differences were observed in almost all evaluation methods between group s 3 (HCS + hADSC) and 5 (HCS + hADSC + PBM), some authors believe that the impacts of stem cell treatment are not affected by the lack of biostimulators.[47,48] Lin et al introduced an innovative method for delivering stem cells by using a combination of chitosan and acellular dermal matrix. This unique system possesses remarkable capabilities for scavenging reactive oxygen species (ROS) and notably mitigating the inflammatory response. By acting as a protective barrier in the presence of a ROS-rich environment, this delivery system effectively eliminates ROS and safeguards MSCs against oxidative stress. Furthermore, it controls the levels of intracellular ROS in MSCs, thereby reducing cellular death induced by ROS. Additionally, this MSC delivery system augments the retention of transplanted stem cells in vivo, stimulates blood vessel formation, and expedites the process of wound healing.[49] Therefore, the positive and significant results observed in group 2 (HCS) could be attributed to the regulation of intracellular ROS levels in MSCs, the reduction of ROS-induced cellular death, the enhanced preservation of transplanted stem cells, the promotion of vessel growth, and accelerated wound healing.[49]

The positive and significant effects observed in group 3 (HCS + hADSC) can be attributed to the additive and combined impacts of stem cell differentiation and their paracrine signaling,[50] along with the beneficial effects of the HCS on the cells within the wound bed.[49] Low-level laser therapy, using PBM, has demonstrated the ability to influence cellular activities, accelerate tissue healing, stimulate cell growth, and facilitate stem cell specialization. This non-invasive approach effectively alleviates pain, reduces inflammation, and supports improved recovery and tissue regeneration.[51] The positive and significant effects observed in group 5 (HCS + hADSCs + PBM) can be attributed to the additive and combined impacts of stem cell differentiation and their paracrine signaling,[43] along with the beneficial effects of the HCS on the cells within the wound bed,[42] as well as the positive effects of PBM on wound bed cells and ADSCs.[51]

There are conflicting results regarding the role of *S. epidermidis* in the injury repairing way. While Leonel et al[52] suggested a positive role for *S. epidermidis* in injury repair, Lindsay et al[53] described it as an invading microorganism. Leonel et al discovered that the cutaneous microbiota act together with cutaneous immune cells, and commensal *S. epidermidis*-induced CD8 + T cells accelerate wound closure by inducing epithelialization.[52] On the other hand, Lindsay et al. stated that the virulence of invading microorganisms and the host's immune status, rather than a high bioburden level alone, affects therapeutic results. Bacteria like *P. aeruginosa, S. aureus,* and *S. epidermidis* possess virulence factors that promote the invasion and destruction of the host tissue, including bacterial proteases.[53]

In conclusion, the combination of HCS, hADSCs, and PBM significantly accelerated the wound healing process compared to individual treatments (HCS alone, hADSCs + HCS, and PBM + HCS) in the maturation phase of injury healing in healthy mice. We propose that additional research should be conducted in human translational studies to explore the potential of the combined approach in reducing inflammation and infection while promoting repairing. Further investigations are required to understand the molecular mechanisms involved in the additive impacts of HCS + hADSCs + PBM in repairing ischemic infected wounds in both healthy and diabetic animals.

Authors' Contribution

Formal analysis: Atarodalsadat Mostafavinia.
Funding acquisition: Abdollah Amini.
Investigation: Houssein Ahmadi, Masoumeh Hajihosseintehrani, Sanaz Alizadeh.
Methodology: Mazaher Gholipourmalekabadi, Fateme Zare, Nafiseh Moeinian.
Project administration: Abdollah Amini.
Resources: Maryam Khodadadi.
Supervision: Abdollah Amini.
Visualization: Mohammadhossein Heidari.
Writing–original draft: Mohammad Bayat, Abdollah Amini.
Writing–review & editing: Sufan Chien, Fatemeh Fadaei Fathabady, Reza Naser.

Competing Interests

The authors declare that they have no conflicts of interest to disclose.

Data Availability Statement

The corresponding authors will supply all information upon reasonable request.

Ethical Approval

After obtaining approval from the Institutional Review Board (IRB) of the School of Medicine at Shahid Beheshti University of Medical Sciences (IR.SBMU.AEC.1402.079), this study was conducted.

Funding

Our research was economically supported by the Research Department of the Medical Faculty at SBMU (Grant No.: 43004222). This article was extracted from the thesis (IR.SBMU.AEC.1402.079)

written by Ms. Masoumeh Hajihosseintehrani.

Informed consent

It was not applicable.

References

1. Sen CK. Human wound and its burden: updated 2022 compendium of estimates. Adv Wound Care (New Rochelle). 2023;12(12):657-70. doi: 10.1089/wound.2023.0150.
2. Sen CK, Roy S, Gordillo G. Wound Healing (Neligan Plastic Surgery: Volume One). Amsterdam: Elsevier; 2017.
3. Guo S, Dipietro LA. Factors affecting wound healing. J Dent Res. 2010;89(3):219-29. doi: 10.1177/0022034509359125.
4. Eming SA, Martin P, Tomic-Canic M. Wound repair and regeneration: mechanisms, signaling, and translation. Sci Transl Med. 2014;6(265):265sr6. doi: 10.1126/scitranslmed.3009337.
5. Najafi R, Chahsetareh H, Pezeshki-Modaress M, Aleemardani M, Simorgh S, Davachi SM, et al. Alginate sulfate/ECM composite hydrogel containing electrospun nanofiber with encapsulated human adipose-derived stem cells for cartilage tissue engineering. Int J Biol Macromol. 2023;238:124098. doi: 10.1016/j.ijbiomac.2023.124098.
6. Moradi S, Alizadeh R, Yazdian F, Farhadi M, Kamrava SK, Simorgh S. A TGF-α and TGF-β1 poloxamer-based micelle/hydrogel composite: a promising novel candidate for the treatment of anosmia. Biotechnol Prog. 2022;38(6):e3294. doi: 10.1002/btpr.3294.
7. Metcalfe AD, Ferguson MW. Bioengineering skin using mechanisms of regeneration and repair. Biomaterials. 2007;28(34):5100-13. doi: 10.1016/j.biomaterials.2007.07.031.
8. Ramhormozi P, Mohajer Ansari J, Simorgh S, Nobakht M. Bone marrow-derived mesenchymal stem cells combined with simvastatin accelerates burn wound healing by activation of the Akt/mTOR pathway. J Burn Care Res. 2020;41(5):1069-78. doi: 10.1093/jbcr/iraa005.
9. Zare P, Pezeshki-Modaress M, Davachi SM, Chahsetareh H, Simorgh S, Asgari N, et al. An additive manufacturing-based 3D printed poly ε-caprolactone/alginate sulfate/extracellular matrix construct for nasal cartilage regeneration. J Biomed Mater Res A. 2022;110(6):1199-209. doi: 10.1002/jbm.a.37363.
10. Leal-Marin S, Kern T, Hofmann N, Pogozhykh O, Framme C, Börgel M, et al. Human amniotic membrane: a review on tissue engineering, application, and storage. J Biomed Mater Res B Appl Biomater. 2021;109(8):1198-215. doi: 10.1002/jbm.b.34782.
11. Han F, Wang J, Ding L, Hu Y, Li W, Yuan Z, et al. Tissue engineering and regenerative medicine: achievements, future, and sustainability in Asia. Front Bioeng Biotechnol. 2020;8:83. doi: 10.3389/fbioe.2020.00083.
12. Krasilnikova OA, Baranovskii DS, Lyundup AV, Shegay PV, Kaprin AD, Klabukov ID. Stem and somatic cell monotherapy for the treatment of diabetic foot ulcers: review of clinical studies and mechanisms of action. Stem Cell Rev Rep. 2022;18(6):1974-85. doi: 10.1007/s12015-022-10379-z.
13. Miana VV, González EA. Adipose tissue stem cells in regenerative medicine. Ecancermedicalscience. 2018;12:822. doi: 10.3332/ecancer.2018.822.
14. Eftekharzadeh M, Simorgh S, Doshmanziari M, Hassanzadeh L, Shariatpanahi M. Human adipose-derived stem cells reduce receptor-interacting protein 1, receptor-interacting protein 3, and mixed lineage kinase domain-like pseudokinase as necroptotic markers in rat model of Alzheimer's disease. Indian J Pharmacol. 2020;52(5):392-401. doi: 10.4103/ijp.IJP_545_19.
15. Mazini L, Rochette L, Admou B, Amal S, Malka G. Hopes and limits of adipose-derived stem cells (ADSCs) and mesenchymal stem cells (MSCs) in Wound Healing. Int J Mol Sci. 2020;21(4):1306. doi: 10.3390/ijms21041306.
16. Qi Y, Dong Z, Chu H, Zhao Q, Wang X, Jiao Y, et al. Denatured acellular dermal matrix seeded with bone marrow mesenchymal stem cells for wound healing in mice. Burns. 2019;45(7):1685-94. doi: 10.1016/j.burns.2019.04.017.
17. Park IS, Chung PS, Ahn JC. Adipose-derived stromal cell cluster with light therapy enhance angiogenesis and skin wound healing in mice. Biochem Biophys Res Commun. 2015;462(3):171-7. doi: 10.1016/j.bbrc.2015.04.059.
18. Jeong GJ, Im GB, Lee TJ, Kim SW, Jeon HR, Lee DH, et al. Development of a stem cell spheroid-laden patch with high retention at skin wound site. Bioeng Transl Med. 2022;7(2):e10279. doi: 10.1002/btm2.10279.
19. Shojaei F, Rahmati S, Banitalebi Dehkordi M. A review on different methods to increase the efficiency of mesenchymal stem cell-based wound therapy. Wound Repair Regen. 2019;27(6):661-71. doi: 10.1111/wrr.12749.
20. Yadav A, Gupta A. Noninvasive red and near-infrared wavelength-induced photobiomodulation: promoting impaired cutaneous wound healing. Photodermatol Photoimmunol Photomed. 2017;33(1):4-13. doi: 10.1111/phpp.12282.
21. Fekrazad R, Asefi S, Allahdadi M, Kalhori K. Effect of photobiomodulation on mesenchymal stem cells. Photomed Laser Surg. 2016;34(11):533-42. doi: 10.1089/pho.2015.4029.
22. Feng P, Luo Y, Ke C, Qiu H, Wang W, Zhu Y, et al. Chitosan-based functional materials for skin wound repair: mechanisms and applications. Front Bioeng Biotechnol. 2021;9:650598. doi: 10.3389/fbioe.2021.650598.
23. Moreira MS, Sarra G, Carvalho GL, Gonçalves F, Caballero-Flores HV, Pedroni ACF, et al. Physical and biological properties of a chitosan hydrogel scaffold associated to photobiomodulation therapy for dental pulp regeneration: an in vitro and in vivo study. Biomed Res Int. 2021;2021:6684667. doi: 10.1155/2021/6684667.
24. Klabukov I, Shestakova V, Krasilnikova O, Smirnova A, Abramova O, Baranovskii D, et al. Refinement of animal experiments: replacing traumatic methods of laboratory animal marking with non-invasive alternatives. Animals (Basel). 2023;13(22):3452. doi: 10.3390/ani13223452.
25. Alizadeh S, Farshi P, Farahmandian N, Aliakbar Ahovan Z, Hashemi A, Majidi M, et al. Synergetic dual antibiotics-loaded chitosan/poly (vinyl alcohol) nanofibers with sustained antibacterial delivery for treatment of XDR bacteria-infected wounds. Int J Biol Macromol. 2023;229:22-34. doi: 10.1016/j.ijbiomac.2022.11.288.
26. Aliakbar Ahovan Z, Khosravimelal S, Eftekhari BS, Mehrabi S, Hashemi A, Eftekhari S, et al. Thermo-responsive chitosan hydrogel for healing of full-thickness wounds infected with XDR bacteria isolated from burn patients: in vitro and in vivo animal model. Int J Biol Macromol. 2020;164:4475-86. doi: 10.1016/j.ijbiomac.2020.08.239.
27. Zare F, Moradi A, Fallahnezhad S, Ghoreishi SK, Amini A, Chien S, et al. Photobiomodulation with 630 plus 810 nm wavelengths induce more in vitro cell viability of human adipose stem cells than human bone marrow-derived stem cells. J Photochem Photobiol B. 2019;201:111658. doi: 10.1016/j.jphotobiol.2019.111658.
28. Moradi A, Kheirollahkhani Y, Fatahi P, Abdollahifar MA, Amini A, Naserzadeh P, et al. An improvement in acute wound healing in mice by the combined application of photobiomodulation and curcumin-loaded iron particles.

Lasers Med Sci. 2019;34(4):779-91. doi: 10.1007/s10103-018-2664-9.
29. Ebrahimpour-Malekshah R, Amini A, Mostafavinia A, Ahmadi H, Zare F, Safaju S, et al. The stereological, immunohistological, and gene expression studies in an infected ischemic wound in diabetic rats treated by human adipose-derived stem cells and photobiomodulation. Arch Dermatol Res. 2023;315(6):1717-34. doi: 10.1007/s00403-023-02563-z.
30. Mostafavinia A, Amini A, Ahmadi H, Rezaei F, Ghoreishi SK, Chien S, et al. Combined treatment of photobiomodulation and arginine on chronic wound healing in an animal model. J Lasers Med Sci. 2021;12:e40. doi: 10.34172/jlms.2021.40.
31. Ebrahimpour-Malekshah R, Amini A, Mostafavinia A, Ahmadi H, Zare F, Safaju S, et al. The stereological, immunohistological, and gene expression studies in an infected ischemic wound in diabetic rats treated by human adipose-derived stem cells and photobiomodulation. Arch Dermatol Res. 2023;315(6):1717-34. doi: 10.1007/s00403-023-02563-z.
32. Sen CK. Human wound and its burden: updated 2020 compendium of estimates. Adv Wound Care (New Rochelle). 2021;10(5):281-92. doi: 10.1089/wound.2021.0026.
33. Hassan WU, Greiser U, Wang W. Role of adipose-derived stem cells in wound healing. Wound Repair Regen. 2014;22(3):313-25. doi: 10.1111/wrr.12173.
34. Riha SM, Maarof M, Fauzi MB. Synergistic effect of biomaterial and stem cell for skin tissue engineering in cutaneous wound healing: a concise review. Polymers (Basel). 2021;13(10):1546. doi: 10.3390/polym13101546.
35. Golchin A, Shams F, Basiri A, Ranjbarvan P, Kiani S, Sarkhosh-Inanlou R, et al. Combination therapy of stem cell-derived exosomes and biomaterials in the wound healing. Stem Cell Rev Rep. 2022;18(6):1892-911. doi: 10.1007/s12015-021-10309-5.
36. Golchin A, Farzaneh S, Porjabbar B, Sadegian F, Estaji M, Ranjbarvan P, et al. Regenerative medicine under the control of 3D scaffolds: current state and progress of tissue scaffolds. Curr Stem Cell Res Ther. 2021;16(2):209-29. doi: 10.2174/1574888x15666200720115519.
37. Teng JY, Guo R, Xie J, Sun DJ, Shen MQ, Xu SJ. [Effects of different artificial dermal scaffolds on vascularization and scar formation of wounds in pigs with full-thickness burn]. Zhonghua Shao Shang Za Zhi. 2012;28(1):13-8. [Chinese].
38. Guo R, Teng J, Xu S, Ma L, Huang A, Gao C. Comparison studies of the in vivo treatment of full-thickness excisional wounds and burns by an artificial bilayer dermal equivalent and J-1 acellular dermal matrix. Wound Repair Regen. 2014;22(3):390-8. doi: 10.1111/wrr.12171.
39. Altman AM, Yan Y, Matthias N, Bai X, Rios C, Mathur AB, et al. IFATS collection: human adipose-derived stem cells seeded on a silk fibroin-chitosan scaffold enhance wound repair in a murine soft tissue injury model. Stem Cells. 2009;27(1):250-8. doi: 10.1634/stemcells.2008-0178.
40. Asgari M, Abdollahifar MA, Gazor R, Salmani T, Khosravipour A, Mahmoudi Y, et al. Photobiomodulation and stem cell on repair of osteoporotic bones. Photobiomodul Photomed Laser Surg. 2022;40(4):261-72. doi: 10.1089/photob.2021.0127.
41. Gazor R, Asgari M, Abdollajhifar MA, Kiani P, Zare F, Fadaei Fathabady F, et al. Simultaneous treatment of photobiomodulation and demineralized bone matrix with adipose-derived stem cells improve bone healing in an osteoporotic bone defect. J Lasers Med Sci. 2021;12:e41. doi: 10.34172/jlms.2021.41.
42. Asgari M, Gazor R, Abdollahifar MA, Fadaei Fathabady F, Zare F, Norouzian M, et al. Combined therapy of adipose-derived stem cells and photobiomodulation on accelerated bone healing of a critical size defect in an osteoporotic rat model. Biochem Biophys Res Commun. 2020;530(1):173-80. doi: 10.1016/j.bbrc.2020.06.023.
43. Khosravipour A, Amini A, Masteri Farahani R, Mostafavinia A, Asgari M, Rezaei F, et al. Evaluation of the effects of preconditioned human stem cells plus a scaffold and photobiomodulation administration on stereological parameters and gene expression levels in a critical size bone defect in rats. Lasers Med Sci. 2022;37(5):2457-70. doi: 10.1007/s10103-022-03509-z.
44. Khosravipour A, Mostafavinia A, Amini A, Gazor R, Zare F, Fallahnezhad S, et al. Different protocols of combined application of photobiomodulation in vitro and in vivo plus adipose-derived stem cells improve the healing of bones in critical size defects in rat models. J Lasers Med Sci. 2022;13:e10. doi: 10.34172/jlms.2022.10.
45. Khosravipour A, Amini A, Masteri Farahani R, Zare F, Mostafavinia A, Fallahnezhad S, et al. Preconditioning adipose-derived stem cells with photobiomodulation significantly increased bone healing in a critical size femoral defect in rats. Biochem Biophys Res Commun. 2020;531(2):105-11. doi: 10.1016/j.bbrc.2020.07.048.
46. Li P, Guo X. A review: therapeutic potential of adipose-derived stem cells in cutaneous wound healing and regeneration. Stem Cell Res Ther. 2018;9(1):302. doi: 10.1186/s13287-018-1044-5.
47. Wu Y, Zhao RC, Tredget EE. Concise review: bone marrow-derived stem/progenitor cells in cutaneous repair and regeneration. Stem Cells. 2010;28(5):905-15. doi: 10.1002/stem.420.
48. Cha J, Falanga V. Stem cells in cutaneous wound healing. Clin Dermatol. 2007;25(1):73-8. doi: 10.1016/j.clindermatol.2006.10.002.
49. Lin W, Qi X, Guo W, Liang D, Chen H, Lin B, et al. A barrier against reactive oxygen species: chitosan/acellular dermal matrix scaffold enhances stem cell retention and improves cutaneous wound healing. Stem Cell Res Ther. 2020;11(1):383. doi: 10.1186/s13287-020-01901-6.
50. Hocking AM, Gibran NS. Mesenchymal stem cells: paracrine signaling and differentiation during cutaneous wound repair. Exp Cell Res. 2010;316(14):2213-9. doi: 10.1016/j.yexcr.2010.05.009.
51. Dompe C, Moncrieff L, Matys J, Grzech-Leśniak K, Kocherova I, Bryja A, et al. Photobiomodulation-Underlying Mechanism and Clinical Applications. J Clin Med. 2020;9(6). doi: 10.3390/jcm9061724.
52. Leonel C, Sena IF, Silva WN, Prazeres P, Fernandes GR, Mancha Agresti P, et al. *Staphylococcus epidermidis* role in the skin microenvironment. J Cell Mol Med. 2019;23(9):5949-55. doi: 10.1111/jcmm.14415.
53. Lindsay S, Oates A, Bourdillon K. The detrimental impact of extracellular bacterial proteases on wound healing. Int Wound J. 2017;14(6):1237-47. doi: 10.1111/iwj.12790.